



Optimised atmospheric pressure CVD of monoclinic VO₂ thin films with picosecond phase transition



Jeffrey M. Gaskell^a, Mohammad Afzaal^{a,*}, David W. Sheel^a, Heather M. Yates^a,
Kaveh Delfanazari^b, Otto L. Muskens^c

^a Materials and Physics Research Centre, University of Salford, Manchester M5 4WT, United Kingdom

^b Optoelectronics Research Centre, University of Southampton, Southampton SO17 1BJ, United Kingdom

^c School of Physics and Astronomy, University of Southampton, Southampton SO17 1BJ, United Kingdom

ARTICLE INFO

Article history:

Received 25 September 2015

Revised 17 December 2015

Accepted in revised form 31 December 2015

Available online 6 January 2016

Keywords:

Dielectric function

Monoclinic

Phase transition

Thermochromics

Vanadium dioxide

ABSTRACT

Monoclinic vanadium oxide (VO₂) thin films with low roughness values were deposited and optimised by atmospheric pressure chemical vapour deposition using vanadium tetrachloride (VCl₄) and water (H₂O). Smooth VO₂ films with good transmittance properties were successfully produced on fluorine doped tin oxide/borosilicate substrates. Systematic investigations confirmed that the quality (including phase) of films being produced strongly depended on substrate, deposition time, temperature, and precursor ratio within the process. Optical characterisation using ellipsometry revealed a strong thermochromic response of the films with a large change in the dielectric function, while time-resolved pump–probe transmission showed the picosecond nature of the phase transition.

© 2016 The Authors. Published by Elsevier B.V. This is an open access article under the CC BY license (<http://creativecommons.org/licenses/by/4.0/>).

1. Introduction

Investigations into the deposition and characterisation of phase-pure monoclinic vanadium dioxide (VO₂) thin films have been of considerable interest predominantly due to their reversible metal–insulator transitions. After heating the material to 68 °C, it converts from monoclinic to more stable rutile phase with a significant optical and conductivity changes. This inherent property of monoclinic phase has made it the choice of material for many applications including transistors [1,2], gas sensing [3], smart windows [4], and optical limiting [5].

A variety of physical and chemical methods such as molecular beam epitaxy [6], pulsed-laser deposition [7], sputtering [8], sol–gel [9], atomic layer deposition [10], ion beam [11], and chemical vapour deposition (CVD) [12] have been studied for growing VO₂ thin films with thermochromic properties. Among CVD processes, atmospheric pressure (AP) CVD technology is highly attractive for growing large area stoichiometric VO₂ thin films with uniform thicknesses and high deposition rates. Moreover, the process is cost competitive and can be integrated into float-glass manufacturing lines. Several research groups including ours have identified growth conditions for depositing only VO₂ thin films in APCVD process [13–18]. The studies have shown that

any variation in growth parameters can profoundly alter both the microstructure and optical properties of deposited thin films.

In this paper, we discuss optimisation of VO₂ thin films by APCVD and resulting properties. For these to be successful, the coating needs to have a number of essential properties. First of all, the coatings should be smooth. The scale of the devices to be deposited on top of the VO₂ coating is of the scale of 20 nm, therefore the surface should preferably have a Root mean square (Rms) roughness of under 10 nm. Secondly, the thermochromic response needs to be large and at a lower temperature than that of bulk value. This is measured in the IR region of the electromagnetic spectrum. Thirdly, the material should exhibit a fast response on the picosecond response scale.

2. Experimental section

The vanadium(IV) chloride (VCl₄), monobutyltin trichloride (MBTC), and trifluoroacetic acid (TFAA) (Sigma Aldrich Ltd) were used as received. Prior to conducting deposition experiments, 1.1 mm borosilicate glass substrates were cleaned with detergent, water, propan-2-ol, and then dried in air. The growth experiments for vanadium oxides were carried out by APCVD, as reported previously [14]. The VCl₄ (as a vanadium source) and H₂O (as oxygen source) were chosen due to their ability to yield favourable growth rates and eliminate any

* Corresponding author.

E-mail address: m.afzaal@salford.ac.uk (M. Afzaal).

inherent carbon sources. Moreover, it was important to purge the system with dry N₂ several times to remove any residual air.

2.1. Thin film deposition

For VO_x deposition, the precursor ratio, the deposition time, and the substrate temperature were varied as summarised in Table 1. To prevent film oxidation, the reactor was allowed to cool down to 100 °C under N₂ before the films were removed. The precursors were transported through the reactor in a stream of N₂ carrier gas.

The fluorine doped tin oxide (FTO) films were deposited using MBTC and TFAA within a designed APCVD coater as described in an earlier publication from our group [19]. The experimental conditions employed have been listed in Table 2. The thickness of the FTO film was set by the number of times the substrate passed under the CVD coating head.

2.2. Characterisation

X-ray diffraction (XRD) patterns were measured on a Siemens D5000 using a Cu K α source. The surface roughness and morphologies were analysed by atomic force microscopy (NanoScope IIIa, Digital Inst. Ltd.). Cross-section scanning electron microscope image was recorded using a Quanta 250 ESEM. The transmission properties of the films were measured on a nkd8000 spectrophotometer (Aquila Instruments Ltd) with an incorporated heating stage. This allows the transmission properties to be measured at set temperatures without the need to move the sample between measurements. Samples were heated in air from room temperature to 75 °C in 5 °C intervals, in order to observe and assess the thermochromic transition. A wavelength range from 800 to 1700 nm was used with s-polarised incident light at an angle of 30°. The film thickness was determined using a Dektak 3ST surface profiler (Veeco) by measuring at least five different points on the step etched film. Before such measurements, films were step etched in 3 M aqueous sodium hydroxide (aq. NaOH) solution for approximately 3 h. Spectroscopic ellipsometry data were collected using a Jobin–Yvon Uvisel-2 variable-angle ellipsometer. Dielectric functions were fitted from the ellipsometry parameters using a Drude–Lorentz model including 4 oscillators. Linear and ultrafast transmission measurements were taken using a picosecond pump–probe spectroscopy setup employing a supercontinuum light source as was used in earlier studies [20]. A pulse picker was used to reduce the repetition rate of the ultrafast pump–probe experiment to 500 kHz to prevent stationary sample heating.

3. Results and discussions

In search for smooth VO₂ thin films with a large thermochromic response, various deposition parameters were systematically investigated by APCVD. The optimum deposition conditions were further used to produce VO₂ films for optoelectronic measurements.

Table 1
Growth parameters utilised for vanadium oxide thin films.

Parameter	Value
Substrate temperature	350–450 °C
VCl ₄ molar flux	5.5×10^{-3} mol/min
H ₂ O molar flux	2.18×10^{-3} – 5.45×10^{-3} mol/min
VCl ₄ :H ₂ O ratio	0.43:1–1.08:1
Deposition time	60–120 s
Flow rate for H ₂ O	0.3 l/min
Flow rate for VCl ₄	0.4 l/min
Total flow	12 l/min

Table 2
Growth parameters utilised for FTO thin films.

Parameter	Value
Substrate temperature	600 °C
MBTC molar flux	5.72×10^{-4} mol/min
TFAA solution concentration	0.2 M
Water:MBTC ratio	5:1
Oxygen flow rate	1.6 l/min
Number of passes	2
Total flow	6 l/min

3.1. Investigation of APCVD parameters

Initial deposition experiments (see Table 1 for details) were conducted directly on the borosilicate glass. Atomic force microscopy (AFM) analysis showed the formation of irregular crystallites with large Rms roughness values for all samples. For example, a typical surface image of a film deposited at 375 °C with a Rms value of 65 nm is given in Fig. 1. The XRD patterns of deposited films showed a peak at ~25° corresponding to (100) peak of orthorhombic V₂O₅ phase (ICDD: 09-0387). As expected, the films showed no thermochromic response.

For the films to be truly functional in optoelectronic devices, it is highly desirable to have smoother films *i.e.* low Rms values and large thermochromic response in IR region. To achieve this it was necessary to deposit VO₂ rather than V₂O₅. As an alternative, 30 nm thick FTO films were deposited on borosilicate glass by APCVD and investigated as template layers for growing smooth VO₂ thin films (see Table 2). The deposited films composed of almost spherical particles with a roughness of 2.3 nm as evident in Fig. S1.

The VO₂ films were deposited on FTO/borosilicate glass between 350–450 °C, with a fixed precursor [VCl₄]:[H₂O] ratio of 0.65. The deposited films were dark yellow and well adherent to the substrates. The grazing XRD measurements showed diffraction peaks corresponding to polycrystalline monoclinic VO₂ (ICDD: 44-0253) regardless of growth temperatures. For example, a film deposited at 375 °C (Fig. 2) showed a peak at 27.86° which could be unambiguously assigned to (011) peak of monoclinic VO₂. The AFM measurements indicated that the deposition temperatures had a profound effect on the roughness of films as their values could be ranged between 8–148 nm (Fig. 3). Interestingly, the films deposited at 375 and 400 °C had roughness values ~10 nm. Whereas, an increase in growth temperature leads to much rougher films that are unacceptable for optoelectronic applications.

When heated, films showed a strong thermochromic response in the IR region below and above transition temperatures at a wavelength of

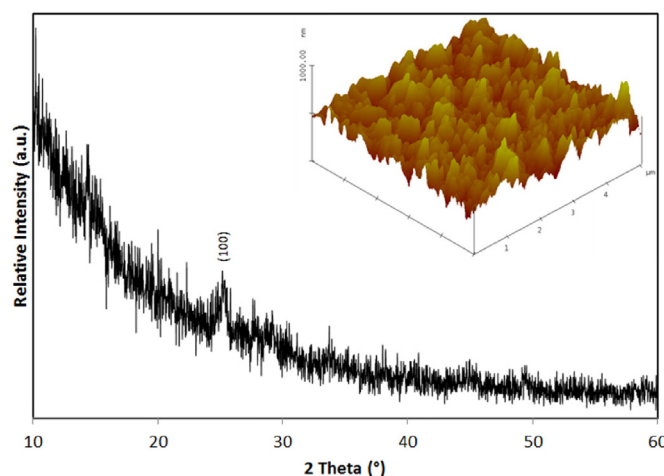


Fig. 1. A typical XRD pattern of V₂O₅ film deposited on borosilicate glass at 375 °C. Inset shows corresponding AFM image with a Rms value of 65 nm.

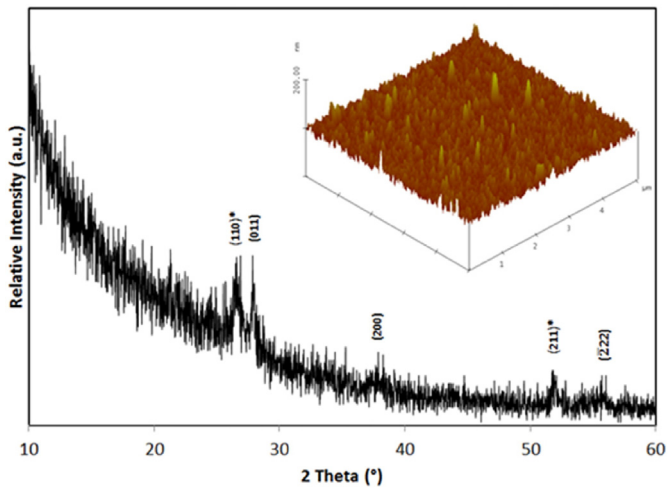


Fig. 2. A typical XRD pattern of VO₂ film deposited on FTO/borosilicate glass at 375 °C for 60 s. Inset shows corresponding AFM image with a Rms value of 6.2 nm. Peaks marked with asterisk are due to the presence of underlying FTO film.

1500 nm. From Fig. 4, it is clearly evident that the transmission values are highly influenced by the deposition temperatures. At low growth temperature *i.e.* 350 °C, the film exhibited a relatively high transmission when measured at room temperature. However, the sample displayed no thermochromic shift. On the contrary, the VO₂/FTO films deposited at higher growth temperatures (>400 °C) did show a marked decrease in IR transmittance. The relative percentage difference in transmission value (Δ_T) was found to be 82.6% for the sample coated at 375 °C.

We speculate that the lack of thermochromic response and relatively high surface roughness for the film deposited at 350 °C may be due to either V₂O₅ or amorphous inclusions. The XRD confirmed the very low level of crystallinity with possibly a mixed oxide. All other samples were shown to be VO₂. A sudden jump in the roughness value for the sample deposited at 450 °C could possibly be a result of substantial increase in precursor decomposition rate. This in turn leads to increased film thickness and hence roughness.

Further experiments were carried out to determine the effect of growth times on the film properties using optimised conditions identified in above experiments. The FTO/borosilicate substrates were set at 375 °C while carrying out the deposition runs for 60, 90 and 120 s. The films were adherent and had good coverage on the substrates. The XRD analysis showed diffraction peaks belonging to both crystalline VO₂ and underlying FTO films (in the case of 60 s) as shown in Fig. 2. As expected, these films became thicker with increased growth times and

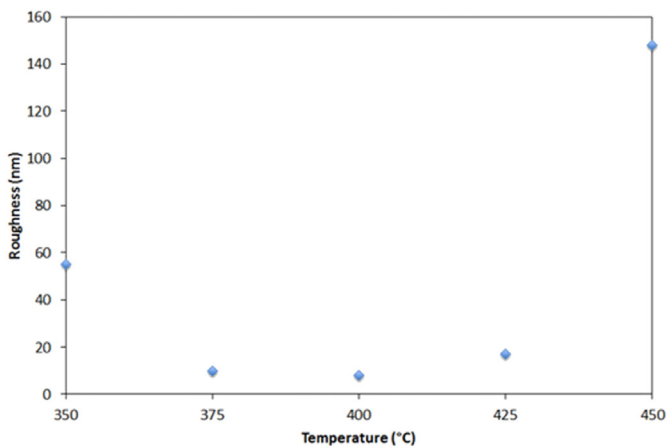


Fig. 3. Roughness values as a function of deposition temperatures while keeping the precursor ratio fixed at 0.65 and deposition time of 60 s.

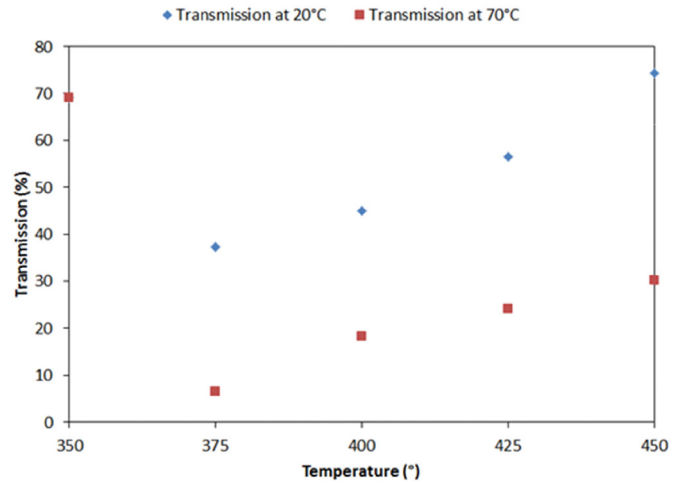


Fig. 4. Transmission values as a function of different deposition temperatures, while keeping the precursor ratio fixed at 0.65 and deposition time of 60 s.

their thicknesses determined by surface profilometer were 36 (± 3), 52 (± 3) and 88 (± 4) nm for 60, 90 and 120 s, respectively (Fig. 5). The obtained value for 60 sec film corresponds well with the thickness estimated by cross section scanning electron microscope image, 45 (± 6) nm (Fig. S2). Observed increased film thicknesses as a functional of deposition times is aligned with previous reported observation for VO₂ thin films [21]. In comparison, the film deposited under identical growth conditions (375 °C, 90 s) on borosilicate glass, albeit V₂O₅, was substantially thicker (320 \pm 19 nm) and rougher (65 nm). Based on this evidence, it can be safely concluded that the type of substrate influences the phase and quality of VO_x being deposited under similar APCVD conditions.

It is found that prolonged growth experiments led to slightly rougher films, with Rms values only ranging from 6.2 to 10.5 nm as the film thickness increased (Table 3). This in turn implies that increasing film thickness (36–88 nm) does not have a profound effect on the roughness properties of the samples. However, resulting samples did show marked thermochromic behaviour and their values significantly reduced in IR region (Fig. S3). The Δ_T values determined were 52.9, 82.6 and 95.9% for 60, 90 and 120 s, respectively (Table 3). This relationship of Δ_T and sample thickness is due to the fact that that transmission depends on both the refractive index and film thickness, in accordance to optical interference theory. This effect for VO₂ thin films was previously reported by Xu et al. [22].

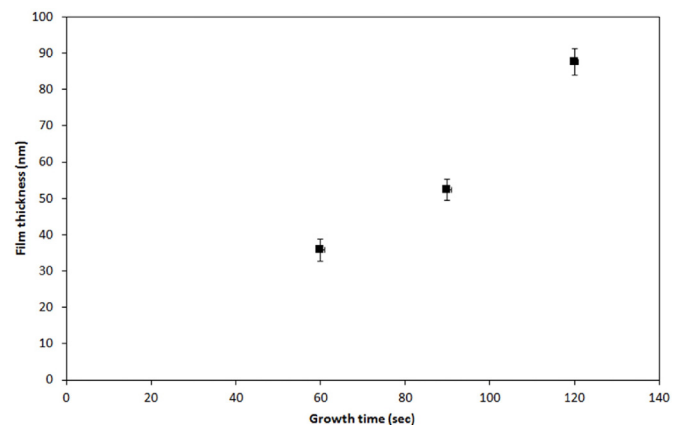


Fig. 5. Film thicknesses at different growth times. Deposited at 375 °C at a precursor ratio of 0.65.

Table 3

Properties of VO₂ thin films at different growth times and oxidations. All samples deposited at 375 °C. Unable to get reliable data for 0.43 ratio.

Growth time (s)	[VCl ₄]:[H ₂ O] ratio	Transmission (%)			Roughness (nm)	Thickness (nm)
		20 °C	70 °C	Δ _T		
60	0.65	62.35	29.35	52.92	6.2	35.78 ± 2.97
90	0.65	37.32	6.49	82.61	9.9	52.32 ± 2.98
120	0.65	40.72	1.65	95.94	10.5	87.68 ± 3.63
60	0.43	88.24	88.06	0.21		
60	0.86	44.14	17.82	59.62	52	104.2 ± 7.9
60	1.08	68.45	65.47	4.36	37.3	82.46 ± 12

It is obvious from the above experiments that under optimised CVD conditions, highly smooth polycrystalline VO₂ films could be deposited on underlying FTO layers. The change in vanadium oxidation state and crystallographic orientation is related to the change in the surface the VO_x was deposited on. This suggests that the presence of a thin polycrystalline FTO layer directs the orientation of the VO_x towards VO₂. A similar structure directing effect has been seen, by us, with APCVD deposition of vanadium oxide over anatase producing mainly a compact granular morphology of mainly V₂O₅ rather than the rod-like VO₂ structure usually formed on glass under those particular deposition conditions [13]. A similar growth observation has been seen for the solution-processed VO₂ on FTO [23] and evaporation of metallic vanadium in oxygen atmosphere [24]. Both FTO and VO₂ have similar rutile type structures, unlike that of orthorhombic V₂O₅, which Zhang et al. [22] attributed to the increased crystallinity and lower deposition temperature of their solution based VO₂ on FTO. According to best of our knowledge, this is the first time that a CVD process has been successfully used for depositing VO₂/FTO/borosilicate coatings with sub 10 nm Rms values.

The [VCl₄]:[H₂O] precursor ratios used during the experiments also had a significant effect on the optical properties of films, due to the formation of VO₂ or V₂O₅. When the VCl₄ was in excess during the process, the film growth was very slow, producing only a very thin film with no thermochromic shift. As the [VCl₄]:[H₂O] ratios increased, the film produced began to exhibit thermochromic shifts and the results are summarised in Table 3. The data is consistent with previous thickness dependent thermochromic properties of VO₂ [22]. The sample grown for 120 s having a [VCl₄]:[H₂O] ratio of 0.65 yielded the greatest Δ_T value of ~96%. The XRD results showed these materials to be composed of VO₂ phase. Increasing the ratio further produced thick films that had no thermochromic shifts. This together with the high amount of oxidant would suggest an increase in the materials oxidation state. This is confirmed by both the shift in film colour from dark green to yellow, and the XRD that the product is V₂O₅. Also noted was the large increase in Rms, which is in line with previous values seen for V₂O₅.

In light of the above results, an optimum VO₂ film on FTO/glass was obtained at 375 °C, [VCl₄]:[H₂O] ratio of 0.65, and deposition time of 60 s. The precursor ratio and time needed balancing against the increase in roughness at the higher ratio and in particular for the higher deposition times. The optimised samples were then used for further optoelectronic investigations.

3.2. Investigation of optoelectronic properties

The main interest of VO₂ for optoelectronics applications lies in the thermochromic response provided by the electronic phase transition. In order to establish the quality of this thermochromic effect for the fabricated samples, spectroscopic ellipsometry was performed over a spectral range covering the visible and near-infrared window. Fig. 6a and b shows resulting values for the ellipsometry parameters Ψ and Δ, for temperature increases from 30 °C to 75 °C and at a constant angle of

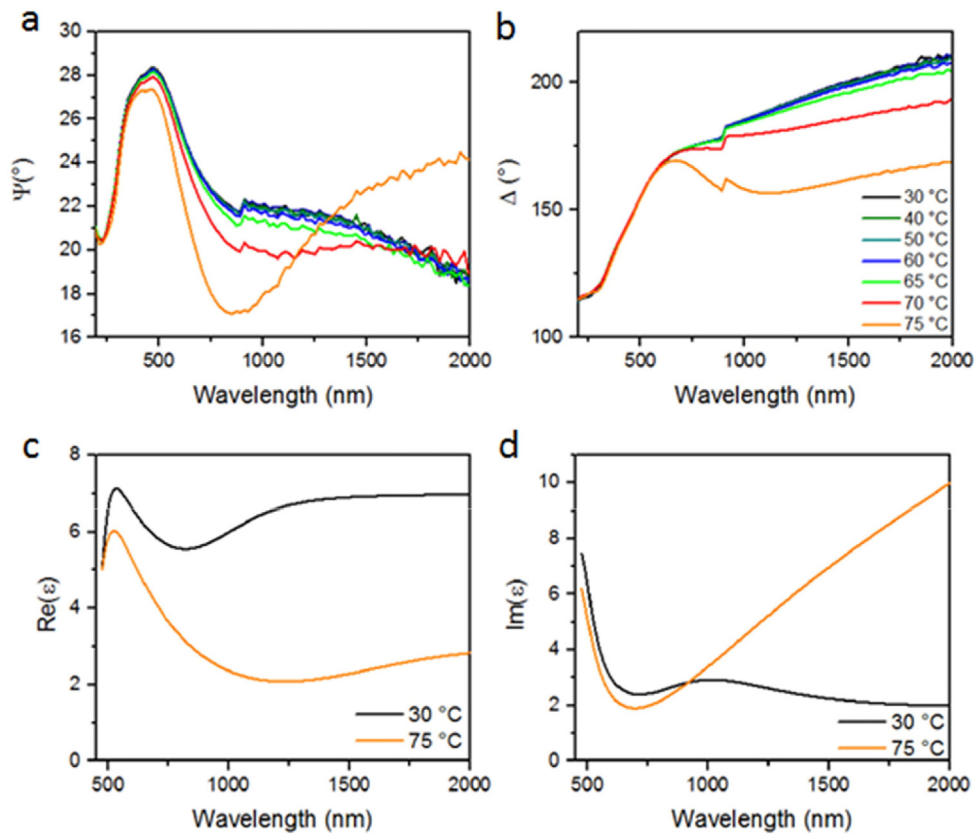


Fig. 6. (a) Ellipsometry parameters Ψ and (b) Δ at different sample temperatures between 30 °C and 75 °C, for an angle of incidence of 55°. (c) Real and (d) imaginary parts of the dielectric function ε at temperatures of 30 °C and 75 °C, obtained using variable-angle spectroscopic ellipsometry.

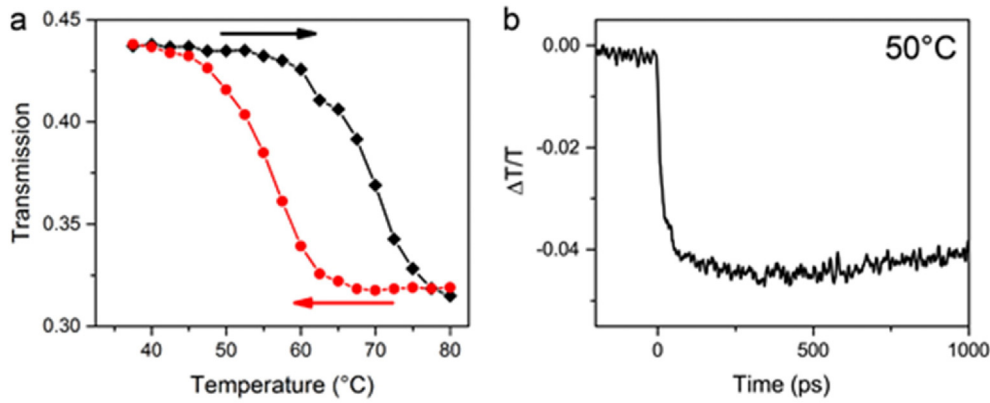


Fig. 7. (a) Temperature dependence of transmission through optimised VO₂ layer with Rms of 6.2 nm showing hysteresis of the phase transition. (b) Time resolved spectroscopy of VO₂ transmission change $\Delta T/T$ at 1500 nm wavelength, showing fast, picosecond nature of the phase transition.

incidence of 55°. It is observed that the optical response remains unchanged up to 65 °C, above which it shows a pronounced modification. Fig. 6c and d shows the dielectric function ϵ extracted from variable angle ellipsometry at 30 °C and 75 °C, for the thin VO₂ layer. A large change in both the real and imaginary parts is observed, associated with the phase transition. While the sample shows a strong decrease in the real permittivity, we do not observe a transition to negative values as found in earlier studies [25]. However, the results are in qualitative agreement with values reported at 75 °C by Kana Kana et al. [26]. Differences in permittivity can be caused by different sample morphologies, ranging from single crystals to polycrystalline thin films, presence of defects, and orientation of the crystallographic axis. In this study it is likely that the increased smoothness of this material is associated with small domain sizes in the range of several nm, which affects the electronic response. Additionally, theoretical studies showed a strong anisotropy of the metallic response, with only one crystallographic direction presenting the metallic response.

The strong thermochromics response of the films is confirmed by optical transmission spectra shown in Fig. S3 (a), showing a large drop in transmission in the metallic state primarily in the near-infrared, with little change in the visible range. The samples show temperature hysteresis behaviour with a width of around 20 °C. (Fig. 7a) Next to direct control of the temperature using a heater stage, the phase transition could also be controlled locally using optical pulses focused onto the sample. Fig. 7b shows the time dynamics of the differential optical

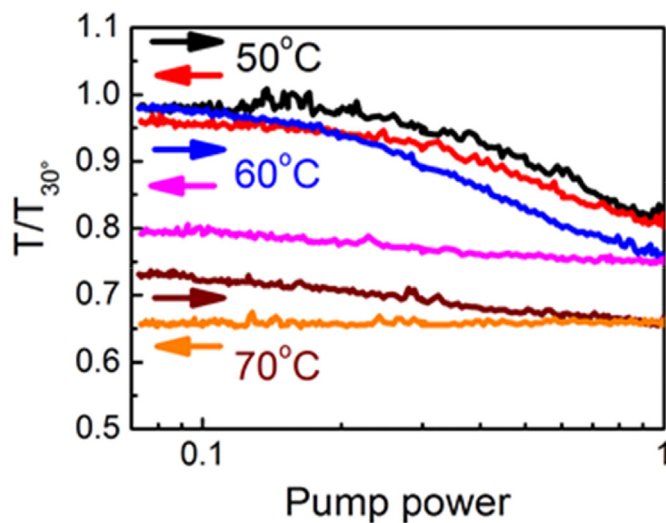


Fig. 8. Optical pumping hysteresis curves against normalized pump power (1.0 corresponds to 10 nJ pulse energy).

transmission $\Delta T/T$ following excitation by a high-intensity (5 nJ) pump laser at 1060 nm wavelength. The pump light was focused on a small area of around 1 μm in diameter, resulting in a local fluence of around 50 mJ/cm^2 . The duration of the pump pulse was 11 ps while the repetition rate was 500 kHz, providing sufficient time between pulses to enable full recovery of the VO₂ by thermal relaxation. The sample temperature was kept at 50 °C, just below the hysteresis loop. Optical pumping results in a very fast excitation of the sample and a concomitant phase change, which reaches approximately 25% of the full modulation achieved using the heater stage. Comparing the reduced switching amplitude with the temperature curve of Fig. 7a indicates that the effect is associated with a local temperature change of several degrees.

Periodic optical pumping requires the sample to relax in-between subsequent excitation cycles. For background temperatures below the hysteresis loop, this can be achieved. However at higher temperatures, it is expected that the sample remains in the switched state. Fig. 8 shows the effect by plotting the optical transmission while the pump power is cycled from several percent up to 100% of the maximum laser power of 10 nJ and back. Meanwhile the background temperature was set to 50 °C, 60 °C and 70 °C. At the temperature of 50 °C, *i.e.* below the hysteresis loop, the optical pumping cycle is nearly fully reversible and the transmission recovers back close to its initial value. At a temperature of 60 °C, the optical pumping induces a slightly larger effect, but the sample does not recover back to its original state. This effect can be explained from Fig. 7a by realizing that the optical pumping induces a local temperature rise of several degrees and thus switching of local domains. However, upon cooling the hysteresis of the phase transition results in a latching of the optical switched state. At the highest background temperature of 70 °C, the sample is almost completely switched even without optical pumping, and almost no additional effect of pumping is observed.

4. Conclusions

It has been successfully demonstrated that thin under-layers of APCVD F-doped tin oxide can be used to direct the formation of very smooth VO₂ films. These films are polycrystalline and by choice of the optimum precursor ratio films with excellent thermochromic shifts could be obtained. The quality of deposited films is further demonstrated by the picosecond response of the phase transition and a large change in the dielectric function.

Acknowledgements

The authors acknowledge financial support from the Engineering and Physical Sciences Research Council (EPSRC), UK through EP/J010758/1 project.

The dataset for this work can be found at <http://dx.doi.org/10.5258/SOTON/385560>.

Appendix A. Supplementary data

Supplementary data to this article can be found online at <http://dx.doi.org/10.1016/j.surfcoat.2015.12.090>.

References

- [1] M. Nakano, K. Shibuya, D. Okuyama, T. Hatano, S. Ono, M. Kawasaki, Y. Iwasa, Y. Tokura, *Nature* 487 (2012) 459–462.
- [2] J. Jeong, N. Aetukuri, T. Graf, T.D. Schladt, M.G. Samant, S.S. Parkin, *Science* 339 (2013) 1402–1405.
- [3] E. Strelcov, Y. Lilach, A. Kolmakov, *Nano Lett.* 9 (2009) 2322–2326.
- [4] (a) J. Zhou, Y. Gao, Z. Zhang, H. Luo, C. Cao, Z. Chen, L. Dai, X. Liu, *Sci. Rep.* 3 (2013) 3029;
(b) M.H. Lee, *Sol. Energy Mater. Sol. Cells* 71 (2002) 537–540.
- [5] L.W. Tutt, T.F. Boggess, *Prog. Quantum Electron.* 17 (1993) 299–338.
- [6] J.W. Tashman, J.H. Lee, H. Paik, J.A. Moyer, R. Misra, J.A. Mundy, T. Spila, T.A. Merz, J. Schubert, D.A. Muller, P. Schiffer, D.G. Schlom, *Appl. Phys. Lett.* 104 (2014) 063104–063105.
- [7] D.H. Kim, H.S. Kwok, *Appl. Phys. Lett.* 65 (1994) 3188–3190.
- [8] G. Fu, A. Polity, N. Volbers, B.K. Meyer, *Thin Solid Films* 515 (2006) 2519–2522.
- [9] N.Y. Yuan, J.H. Li, C.L. Lin, *Appl. Surf. Sci.* 191 (2002) 176–180.
- [10] A.P. Peter, K. Martens, G. Rampelberg, M. Toeller, J.M. Ablett, J. Meersschaut, D. Cuypers, A. Franquet, C. Detavernier, J.-P. Rueff, M. Schaeckers, S.V. Elshocht, M. Jurczak, C. Adelman, I.P. Radu, *Adv. Funct. Mater.* 25 (2015) 679–686.
- [11] K. West, J. Lu, J. Yu, D. Kirkwood, W. Chen, Y. Pei, J. Claassen, S. Wolf, *J. Vac. Sci. Technol. A* 26 (2008) 133–139.
- [12] (a) M.B. Sahana, M.S. Dharmaprakash, S.A. Shivashankar, *J. Mater. Chem.* 12 (2002) 333–338;
(b) D. Louloudakis, D. Vernardou, E. Spanakis, S. Dokianakis, M. Panagopoulou, G. Raptis, E. Aperathitis, G. Kiriakidis, N. Katsarakis, E. Koudoumas, *Phys. Status Solidi C* 12 (2015) 856–860;
(c) D. Vernardou, D. Louloudakis, E. Spanakis, N. Katsarakis, E. Koudoumas, *Adv. Mater. Lett.* 6 (2015) 660–663.
- [13] P. Evans, M.E. Pemble, D.W. Sheel, H.M. Yates, *J. Photochem. Photobiol. A* 189 (2007) 387–394.
- [14] D. Vernardou, M.E. Pemble, D.W. Sheel, *Chem. Vap. Depos.* 12 (2006) 263–274.
- [15] T.D. Manning, I.P. Parkin, R.J.H. Clark, D. Sheel, M.E. Pemble, D. Vernardou, *J. Mater. Chem.* 12 (2002) 2936–2939.
- [16] T.D. Manning, I.P. Parkin, *Polyhedron* 23 (2004) 3087–3095.
- [17] D. Vernardou, D. Louloudakis, E. Spanakis, N. Katsarakis, E. Koudoumas, *Sol. Energy Mater. Sol. Cells* 128 (2014) 36–40.
- [18] D. Louloudakis, D. Vernardou, E. Spanakis, N. Katsarakis, E. Koudoumas, *Surf. Coat. Technol.* 230 (2013) 186–189.
- [19] H.M. Yates, P. Evans, D.W. Sheel, S. Nicolay, L. Ding, C. Ballif, *Surf. Coat. Technol.* 13 (2012) 167–174.
- [20] Y. Wang, M. Abb, S.A. Boden, J. Aizpurua, C.H. de Groot, O.L. Muskens, *Nano Lett.* 13 (2013) 5647–5653.
- [21] L.-K. Tsui, H. Hildebrand, J. Lu, P. Schmuki, G. Zangari, *Appl. Phys. Lett.* 13 (2013) 202102-1–2202102-4.
- [22] G. Xu, P. Jin, M. Tazawa, K. Yoshimura, *Jpn. J. Appl. Phys.* 43 (2004) 186–187.
- [23] Z. Zhang, Y. Gao, H. Luo, L. Kang, Z. Chen, J. Du, M. Kanehira, Y. Zhang, Z.L. Wang, *Energy Environ. Sci.* 4 (2011) 4290–4297.
- [24] A. Atrei, T. Cecconi, B. Cortigiani, U. Bardi, M. Torrini, G. Roviida, *Surf. Sci.* 513 (2002) 149–162.
- [25] H.W. Verleur, A.S. Barker, C.N. Berglund, *Phys. Rev.* 172 (1968) 788.
- [26] J.B. Kana Kana, J.M. Ndjaka, V. Vignaud, A. Gibaud, M. Maaza, *Opt. Commun.* 284 (2011) 807–812.